# Optimization of tapered capillary optics for use at the Microfocus Beamline (ID13) at the European Synchrotron Radiation Facility (ESRF)

L. Vincze, K. Janssens and F. Adams
*Dept. of Chemistry, University of Antwerp, Belgium*

A. Rindby
*Chalmers University of Technology, Göteborg, Sweden*

P. Engström and C. Riekel
*European Synchrotron Radiation Facility, Grenoble, France*

## Abstract

Using a detailed 3-dimensional ray-tracing code for the modeling of capillary optics the optimum dimensions of linearly tapered glass capillaries have been calculated for the Microfocus beamline (ID13) of the ESRF. The aim of the calculations was to further improve the performance of this optical element which is used routinely at ID13 as a post-focusing device. That is, to reduce the currently available beam size of 2 $\mu m$ down to the sub-micron level while retaining the highest possible photon intensity. Three target beam sizes are considered in the following studies: 1.0, 0.5 and 0.1 $\mu m$ for which cases the optimum length and entrance diameter values have been determined yielding maximum output photon intensities, assuming conical capillary shapes.

## Introduction

A simple way of concentrating hard X-ray beams to micron size is offered by tapered glass capillaries which employ the principle of multiple total external reflections to guide the photons along the device. A photon beam entering the capillary is reduced in size which is comparable to that of the exit diameter of the glass tube [1-9].

A given ray which enters the capillary follows a three dimensional, multiple bounce trajectory that is basically determined by the shape of the device and the initial conditions of the ray. As long as the reflection angles of the photon along its trajectory remain below the critical angle of total reflection $\theta_C(E)$, which is determined by the photon energy $E$ and the composition of the reflecting material, the ray is transmitted through the device with relatively high efficiency. While the beam transmission properties of ideal capillary shapes (coupled with point X-ray sources), such as parallel bore hole, linearly tapered or ellipsoidal

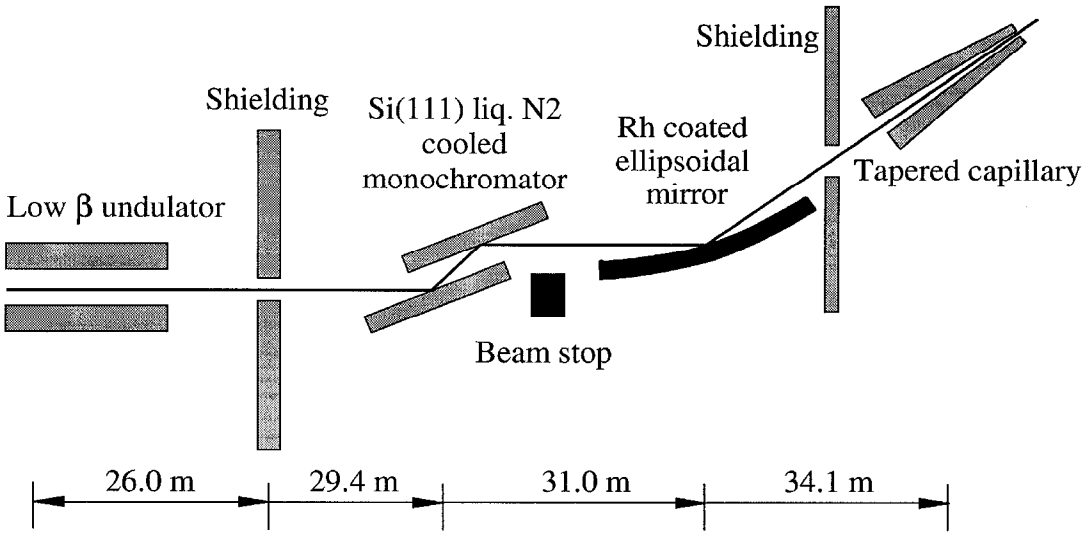


Fig.1.Schematic drawing of the Microfocus beamline at the ESRF (ID13). The primary X-ray beam originates from a low beta undulator. After monochromatization the synchrotron beam is focused by an ellipsoidal mirror onto the entrance of a tapered capillary.

capillaries, can be described by analytical models [10-12], one needs to apply a three dimensional ray-tracing method for characterizing more complex situations [13-15]. The necessity to use a three dimensional model immediately arises when considering the situation represented by the setup at the Microfocus beamline (ID13) of the ESRF (see Fig.1).

As illustrated in Fig.1, an extended X-ray source (i.e., a focusing mirror) is located relatively close to the capillary entrance (see detailed description in the experimental section), resulting in helical photon trajectories instead of simple two-dimensional planar propagation. A typical photon trajectory for this case is shown in Fig.2, which clearly illustrates the truly three dimensional nature of the photon propagation within the glass tube. As illustrated here, even for an ideal conical capillary shape, the number of reflections involved can be substantially higher than that suggested by a simple two-dimensional description of photon propagation. In order to cover the special case of the converging incident beam focused by the ellipsoidal mirror onto the entrance of the tapered capillary a detailed three-dimensional ray-tracing code, developed at the University of Antwerp, has been used [15].

In the first part of the paper, an example is given to illustrate the ability of the code to predict the far-field image (i.e., the angular distribution) of the beam generated at this beamline by an existing tapered capillary. Next, experimental photon intensities through a tapered capillary and a pinhole are compared to values predicted by the ray-tracing code. After these examples, the optimum dimensions of conical capillaries are determined for this particular configuration of low-β undulator - ellipsoidal mirror - capillary optics, present at the Microfocus beamline.

 

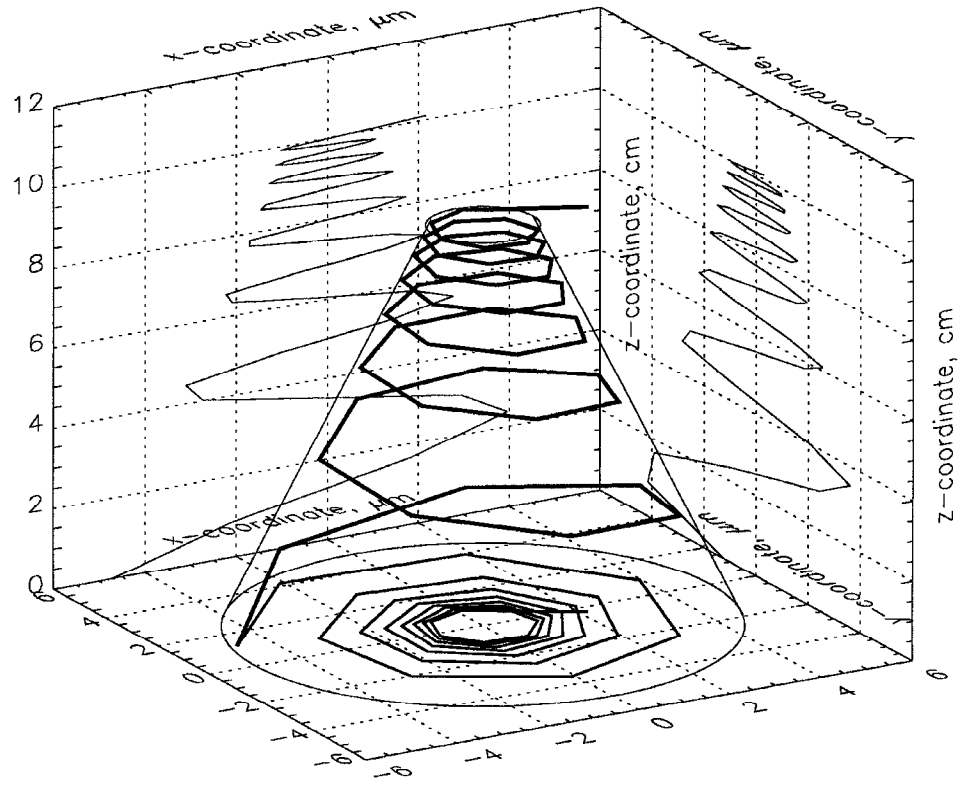


Fig.2 Typical photon trajectory obtained by the simulation code through a conical capillary tapering from 10 $\mu m$ to 2 $\mu m$ along a length of 10 *cm*.

## Experimental Setup

At the Microfocus beamline of the ESRF (ID13), shown schematically in Fig.1, tapered glass capillaries have routinely been used as add-on optics to produce an X-ray micro beam with sizes down to 2 $\mu m$ and intensities over $10^{10}$ $ph/s/\mu m^2$ at an energy of 13 *keV* within an energy bandwidth of $\Delta E/E \approx 2\times10^{-4}$ [16,17]. The primary X-ray source employed here is a low beta undulator with a source size of 0.139 x 0.026 $mm^2$ (HxV FWHM) and divergencies of 0.233 x 0.020 $mrad^2$ (HxV FWHM). The undulator beam, after monochromatization by a $LN_2$-cooled Si(111) channel-cut monochromator, is focused by a Rh coated ellipsoidal mirror located at a distance of 31 *m* from the source having a theoretical demagnification of 10. This mirror produces a photon beam with sizes of 16 x 27 $\mu m^2$ (HxV FWHM) and divergencies of 2.4 x 0.3 $mrad^2$ (HxV FWHM) with an overall intensity of about $10^{13}$ *ph/s* at 13 *keV*. The focused photon beam is further concentrated down to the 2 $\mu m$ level using a tapered glass capillary.

 

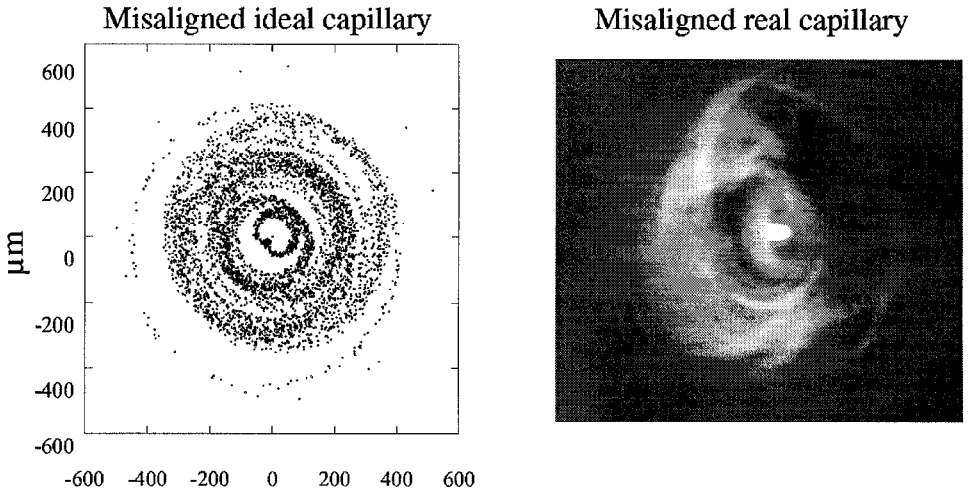


Fig.3 Simulated and experimental output images of a misaligned tapered capillary having a length of 10 *cm*, reducing the beam from 100 $\mu m$ to 10 $\mu m$. The experimental image was recorded at the Microfocus beamline of the ESRF (ID13).

## Experiment vs. simulation

Fig.3 shows a comparison of experimental and simulated output images of a glass capillary, having a length of 10 *cm*, tapering from 100 $\mu m$ to 10 $\mu m$. The output pattern was recorded by a CCD camera at a distance of 5 *cm* from the capillary exit.

This far-field image of the output beam is fully determined by the angular distribution of the beam leaving the capillary. There are several distorted rings that can be discerned in the image, corresponding to different reflection orders of the photon beam travelling through the device. For an ideal conical capillary, aligned perfectly with the source, the output pattern would consist of regular, concentric rings [15]. In this case, however, due to the imperfect alignment and non-ideal capillary shape, the rings suffer considerable distortions.

## Experimental capillary efficiency and gain factor

Compared to a simple pinhole collimation of the beam produced by the mirror, the use of capillary optic yields a (measured) flux density gain at this beamline of about 4 at the exit end of the capillary. This flux density gain was achieved using a tapered capillary with an entrance diameter of 77 $\mu m$, reducing the beam diameter to 2 $\mu m$ along its length of 12.3 *cm*.

The flux density gain could be determined by measuring the photon flux at the exit end of the capillary and comparing it with the flux value obtained for a collimator. The latter was a 20 *mm* long, cylindrical collimator consisting of 3 pinholes with 10 *mm* spacing, each having a diameter of 10 $\mu m$. The measured flux corresponding to the capillary was $3.4\times10^{10}$ *ph/s* (within a 2 $\mu m$ spot) at 100 *mA* ring current at the photon energy of 13 *keV* while the photon

flux behind the 10 $\mu m$ collimator was determined to be $2.1\times10^{11}$ *ph/s* under the same conditions. After normalizing these values with the generated beam sizes, 2 $\mu m$ for the capillary and 10 $\mu m$ for the collimator, the flux density gain was calculated to be about 4.

## Optimization of conical capillary dimensions

*Capillary length optimization*

The simplest type of tapered capillary is represented by the ideal conical shape which can geometrically be characterized by its entrance and exit diameters and its length. Being a non-imaging X-ray concentrator, this device produces a beam whose size is fully determined by its exit diameter and by the distance of the observation point from the capillary tip, independently from the size of the X-ray source. In the following calculations three target resolutions are considered, determining the exit diameters of the designed capillaries to be (a) 1 $\mu m$, (b) 0.5 $\mu m$ and (c) 0.1 $\mu m$. Note that due to the considerable divergency of the generated capillary beam (which can roughly reach twice the critical angle, i.e., 4.6 *mrad* at 13 *keV*), the achieved beam sizes will always be larger on the sample than the above cases suggest, because of the non-zero sample-capillary distance. In practice, this distance cannot be smaller than 50-100 $\mu m$.

In order to determine the optimum length of the ideally conical shaped capillaries concentrating the mirror beam down from 30 $\mu m$ (entrance diameter) to the exit diameters listed under the cases (a)-(c), the photon throughput as a function of capillary length was calculated for each case. Figs.4.a-c show the calculated transmission efficiencies for 13 *keV* photons for the above mentioned three output diameters, assuming that the capillary entrance is placed in the focal plane of the mirror and is perfectly aligned with the incoming beam.

The capillary material in all of these calculations was assumed to be borosilicate glass having different surface roughness values, that is, 0, 30 and 60 Å. Since the entrance diameter is fixed in all of these cases (i.e., 30 $\mu m$), the input photon flux, captured by the capillary entrance, remains the same for each case and is calculated to be 73.3 % of the full mirror beam that is $7.3\times10^{12}$ *ph/s*. Using this value, the expected output fluxes (at 13 *keV*) could be directly calculated for the various capillary exit openings as the function of capillary length and are shown in Figs.4.a-c.

A very interesting conclusion of these calculations is that the optimum length values are practically the same independently of the exit diameter of the capillary,. This is actually the consequence of the fact that the assumed entrance diameter (30 $\mu m$) is much larger than the exit diameter values considered here (i.e., 1.0, 0.5 and 0.1 $\mu m$), meaning that the cone angle of the capillary will barely change for these cases.

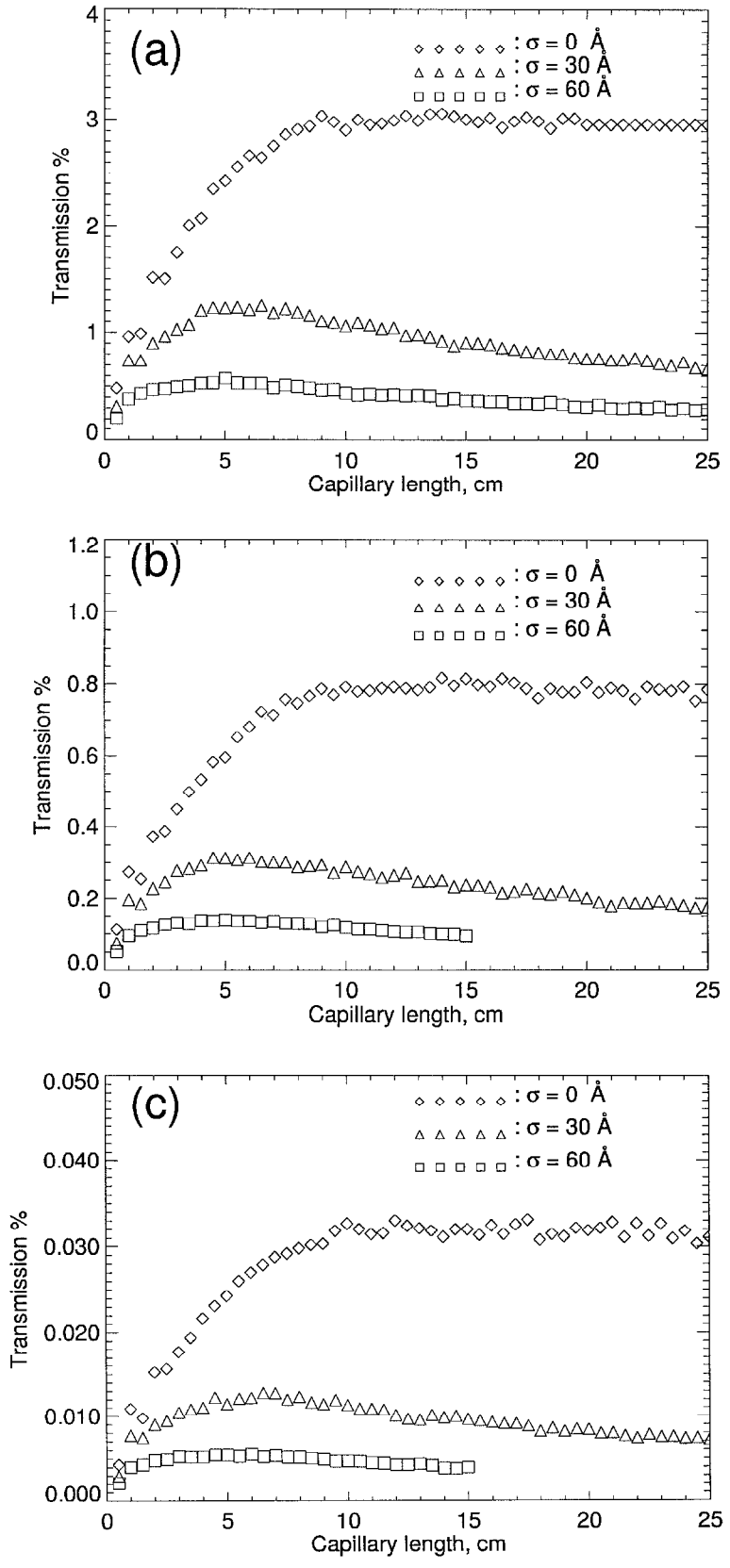


Fig.4. Calculated transmission efficiencies at a photon energy of 13 *keV* as the function of capillary length in case of ideal conical capillaries. In the calculations three surface roughness values were considered, (i.e., σ= 0, 30 and 60 Å), indicated by the different symbols. The devices were assumed to taper from 30 $\mu m$ to (a) 1 $\mu m$, (b) 0.5 $\mu m$ and (c) 0.1 $\mu m$.

As the optimum capillary length is mainly dependent on the capillary cone angle, it will not change significantly when going from 1.0 $\mu m$ to 0.1 $\mu m$ in exit diameter. However, the maximum transmission at the optimal length corresponding to a perfect reflecting surface is reduced from 3.1 % to 0.033 % when decreasing the exit diameter from 1.0 $\mu m$ to 0.1 $\mu m$.
For ideally smooth inner surfaces (zero roughness) the optimal length, producing the highest output photon intensity, is about 12-13 *cm* whereas for non-zero surface roughnesses shorter capillaries are favoured, with optimal length values in the range of 5-6 *cm*. This is not very surprising as the reduced reflectivity (due to the roughness) requires the reduction of the number of reflections, yielding smaller optimum capillary lengths.
The expected photon intensities at 13 *keV* for the three different capillaries are fairly high, even for the largest surface roughness value of 60 Å which was considered here, reaching intensities in the range of $4.2\times10^{10}$, $1.0\times10^{10}$ and $4.0\times10^{8}$ *ph/s* in case of the exit openings of 1.0, 0.5 and 0.1 $\mu m$, respectively.
Table 1. summarizes the predicted optimum capillary flux density gain factors at the X-ray energy of 13 *keV* for the various capillaries and surface roughness values.

Table 1. Calculated photon intensities and gain factors at 100 *mA* ring current for different surface roughnesses and exit diameters corresponding to ideal conical profiles, tapering from 30 $\mu m$ to 1 $\mu m$ (capillary A), 0.5 $\mu m$ (capillary B) and 0.1 $\mu m$ (capillary C). All capillary lengths were assumed to be 12 *cm* for zero and 5 *cm* for non-zero roughness.

| | Capillary A | | Capillary B | | Capillary C | |
|---|---|---|---|---|---|---|
| Surface roughness [Å] | Intensity [ph/s] | Gain | Intensity [ph/s] | Gain | Intensity [ph/s] | Gain |
| 0 | $2.19\times10^{11}$ | 26.0 | $5.79\times10^{10}$ | 27.6 | $2.41\times10^{9}$ | 39.3 |
| 30 | $8.96\times10^{10}$ | 10.7 | $2.28\times10^{10}$ | 10.8 | $8.36\times10^{8}$ | 9.9 |
| 60 | $4.20\times10^{10}$ | 5.0 | $1.01\times10^{10}$ | 4.8 | $3.97\times10^{8}$ | 4.7 |

*Capillary entrance diameter optimization*

In order to further improve the performance of the above capillaries, the entrance diameters have also been optimized by the ray-tracing code for the 1.0 and 0.5 $\mu m$ exit diameter cases. Next to the fixed exit diameter, the length of the given capillary was also fixed at the optimum value determined in the previous section, that is, 12 *cm* for zero and 5 *cm* for non-zero surface roughness values. The latter length proved to be a good choice for both 30 and

60 Å surface roughness values, as the optimum length did not change significantly above σ=30 Å.

When optimizing the entrance diameter with respect to the achievable output photon flux, one has to keep in mind that on the one hand the photon intensity captured by the capillary is increasing as long as the entrance diameter is smaller than the size of the incident beam. The exact dependence of the captured flux on the entrance diameter is determined by the spatial distribution of the photon beam at the capillary entrance which in this case was assumed to be a Gaussian distribution. On the other hand, increasing the entrance diameter causes the transmission efficiency of the capillary to decrease. As a result of this, the output photon flux (being the product of the captured flux and the efficiency) has a well-defined maximum at a given entrance diameter depending on the source distribution, where the diameter is not greater than the size of the full beam. A larger capillary opening than that of the beam size would only decrease the efficiency without collecting more photons resulting in the loss of output intensity. Fig.5 illustrates the results corresponding to the entrance optimization of the capillaries having exit diameters of 1.0 and 0.5 μm, where the predicted output intensity is shown as the function of entrance diameter for 0, 30 and 60 Å surface roughness.

As illustrated by these figures, the optimum entrance diameter increases when the surface roughness increases: the loss in average reflectivity is counterbalanced by the gain due to the larger fraction of the incident beam being collected by the capillary. This dependency is fairly weak in the case of the capillary having an opening of 1 μm in where the optimum entrance diameter is varying only between 17 and 18 $\mu m$ for all surface roughness values. It becomes more important for the device having a smaller exit diameter (0.5 $\mu m$) where the optimum entrance diameter changes from 13 to 17 $\mu m$ when the roughness increases from zero to 60Å. When comparing the output fluxes with the case of the capillaries with 30 $\mu m$ entrance diameter, the optimization of the entrance diameter results in an average increase of about 50 % with respect to the output photon intensity.

## Conclusions

In this work the optimum capillary dimensions were determined for use as a second stage X-ray concentrator at the Microfocus beamline (ID13) of the ESRF. In the calculations experimentally determined source parameters were used which were measured in the focal plane of the focusing mirror. This mirror serves as the actual X-ray source for the glass capillary.

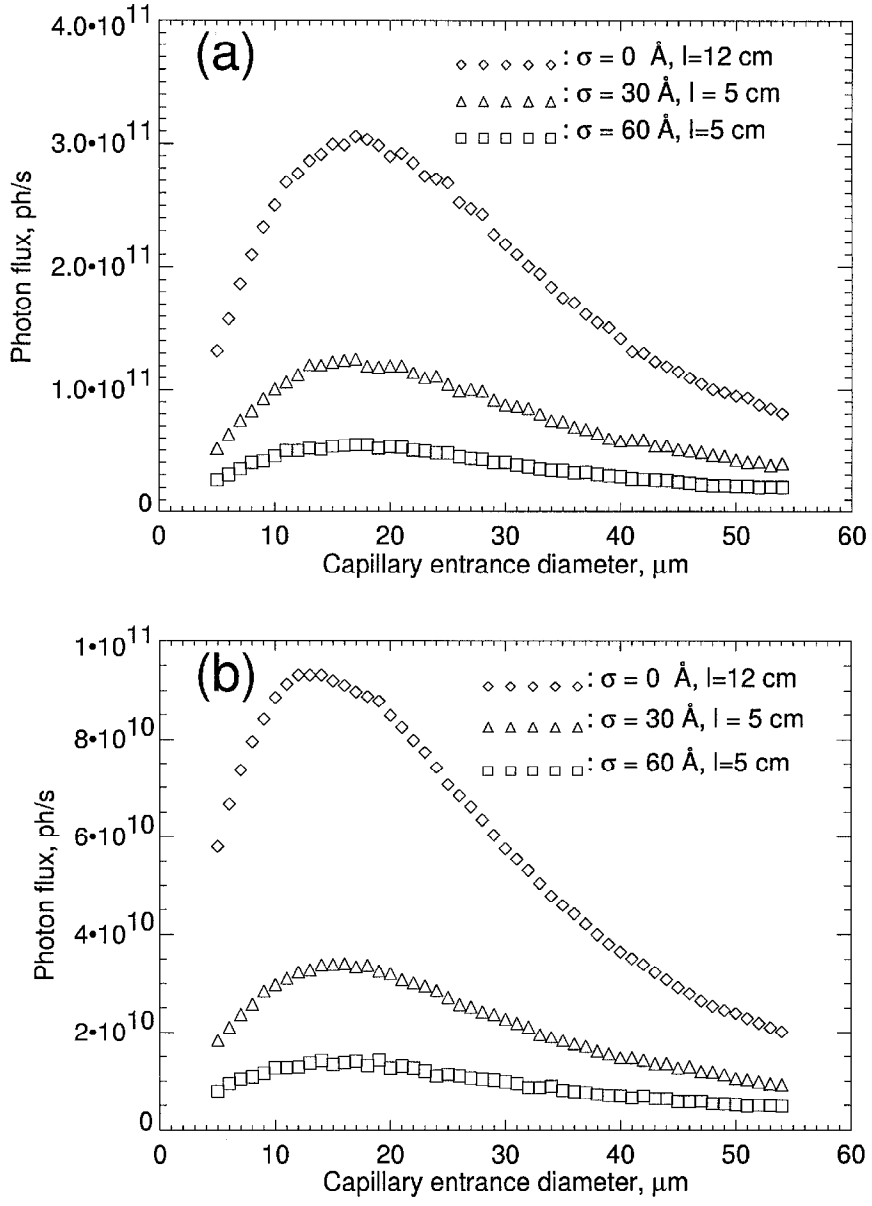


Fig.5 Calculated photon fluxes at 13 *keV* for ideal conical capillaries as the function of entrance opening for surface roughness values of σ = 0, 30 and 60 Å. The capillary length was assumed to be 5 *cm* and the exit diameter was (a) 1 *μm* and (b) 0.5 *μm*.

Three target resolutions were considered: 1, 0.5 and 0.1 *μm*, respectively. For all of these exit diameters, at 13 *keV* X-ray energy, the optimum length of the capillaries varies between 12 and 13 *cm* when ideally smooth inner glass surface is assumed. The optimum length (5-6 *cm*) is considerably shorter for rough surfaces, and is nearly independent from the roughness value in the range of 30-60 Å.

## Acknowledgements

L. Vincze and K. Janssens are fellows of the Belgian National Science Fund (FWO).

## References

[1] D.H. Bilderback, S.A. Hoffmann and D.J. Thiel, *Science*, **263**, 14 (1994).

[2] D.J. Thiel, E.A. Stern, D.H. Bilderback, A. Lewis, *Physica B*, **158**, 314 (1989).

[3] D.J. Thiel, D.H. Bilderback, A. Lewis, E.A. Stern, *Nucl. Instrum. Methods*, **A317**, 597 (1992).

[4] S.A. Hoffman, D.J. Thiel, D.H. Bilderback, *Nucl. Instrum. Methods*, **A347**, 384 (1994).

[5] D. H. Bilderback, D. J. Thiel, R. Pahl, and K. E. Brister, *J. Synchr. Rad.*, **1**, 37 (1994).

[6] P. Engström, S. Larsson, A. Rindby, A. Buttkewitz, S. Garbe, G. Gaul, A. Knöchel and F. Lechtenberg, *Nucl. Instrum. Methods,* **A302**, 547 (1991).

[7] E.A. Stern, Z. Kalman, A. Lewis, K. Liebermann, *Applied Optics*, **27**, 5135 (1988).

[8] K.H. Kim, D.L. Brewe, F.C. Brown, E.A. Stern, *Rev. Sci. Instrum.*, **67 (9)**, (1996).

[9] K.F. Voss, K.H. Kim, E.A. Stern, F.C. Brown, S.M. Heald, *Nucl. Instrum. Methods*, **A347**, 390 (1994).

[10] A. Kuczumov, S. Larsson, *Applied Optics*, **33**, 7928 (1994).

[11] D.X. Balaic, K.A. Nugent, *Applied Optics*, **34**, No. 31, 7263 (1995).

[12] G.S. Cargill III, K. Hwang, J.W. Lam, P.-C. Wang, E. Liniger, I.C. Noyan, *SPIE Proceedings*, 2516 (1995).

[13] F.C. Brown, K.H. Kim, S.M. Heald, B.M. Barg, E.A. Stern, *Rev. Sci. Instrum.*, **67 (9)**, (1996).

[14] L. Vincze, K. Janssens and F. Adams, *Adv. X-ray Anal.*, **37**, 563 (1994).

[15] L. Vincze, K. Janssens, F. Adams and A. Rindby, *X-ray Spectrometry*, **24**, 27 (1995).

[16] P. Engström, C. Riekel, C.H. Chanzy, *ESRF Newsletter* (1995).

[17] P. Engström, C. Riekel, *J. Synchr. Rad.*, 3, **97** (1996).